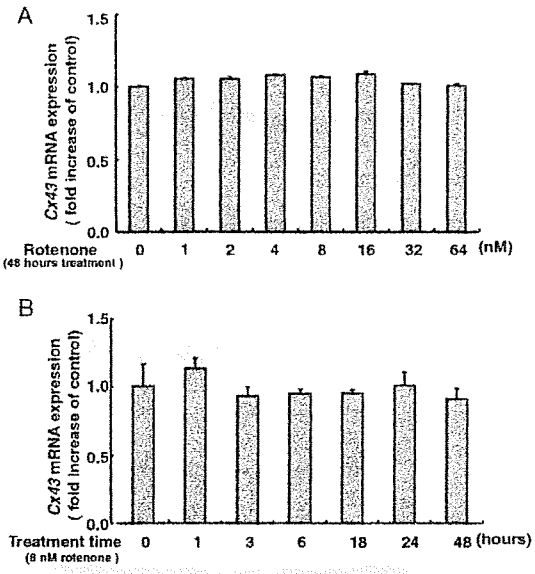

Fig. 2. Real-time RT-PCR analysis of *Cx43* mRNA expression. Astrocytes were cultured with or without rotenone for 48 h at the indicated concentrations (A) or with 8 nM rotenone for the indicated times (B). The value of untreated astrocytes (control) was taken as unity to calculate the fold increase. *Cx43* mRNA levels were normalized by *GAPDH* mRNA, whose level did not change during culture with rotenone (data not shown). Results are means of at least three experiments. Values are mean±SE.

along the plasma membrane between cells (Fig. 1Ba'). Enhanced total Cx43 foci were co-localized with phosphorylated Cx43 (Fig. 1Bd') in the rotenone-treated cells. These results suggest that upregulation and trafficking of Cx43 protein to the membrane were induced by rotenone.

Rotenone enhanced GJIC through Cx43 in cultured astrocytes

We next examined the effect of rotenone on GJIC in cultured astrocytes. The GJIC was assessed by the FRAP technique, in terms of the RR. After photobleaching, sequential scans detected the recovery of fluorescence in the bleached cells as the dye was transferred to photobleached cells through GJIC from surrounding non-bleached cells. The RR at 48 h of treatment showed a dose-dependent increase up to 8 nM rotenone, although this was followed by a slight decrease (Fig. 3A). Further, time course analysis showed a time-dependent increase in GJIC after rotenone treatment (Fig. 3B). These results suggest that rotenone treatment of cultured astrocytes generated increased protein levels and a broadened membrane distribution of Cx43, which in turn led to enhancement of GJIC.

Total and phosphorylated Cx43 protein levels were enhanced in astrocytes in the rat PD model

To investigate whether Cx43 levels may be altered in Parkinsonism, we examined the Cx43 protein level and immunoreactivity in our rotenone-induced rat PD model. In this model, chronic exposure to rotenone remarkably reduced TH immunoreactivity in the substantia nigra pars compacta (SNc), the same area where loss of DA neurons occurs in human PD (Supplementary Fig. 1). Fig. 6 shows that Cx43 was found in all regions, though at different levels, and that the Cx43 protein level was significantly lower in striatum than in other brain regions (Fig. 4), though the P_1 and P_2 forms of Cx43 were markedly enhanced in striatum of the treated group. Significant differences of total Cx43 levels were found in striatum of rotenone-treated rats at 1, 2, and 4 weeks, as well as in hippocampus of rotenone-treated rats at 1 week. However, no significant changes were observed in other regions (Fig. 5A, B). Next, Cx43 immunohistochemistry was performed on the SN and striatum and globus pallidus (GP) of vehicle- or rotenone-treated rats (Fig. 6). In the SN, Cx43 immunoreactivity was enhanced in rotenone-treated rats compared with that in vehicle-treated rats. Elevation of Cx43 was more noticeable in substantia nigra pars reticulata (SNr) than in SNc (Fig. 6A). Increase of Cx43 after rotenone treatment was more pronounced in GP than striatum (Fig. 6B).

SNc and striatum in rotenone-treated rats revealed DA neuronal loss when visualized by TH immunoreactivity (Fig. 6), consistent with previous observations (Betarbet et al., 2000). Interestingly, the degree of enhancement of Cx43 by rotenone was found to be lower in SNc and striatum than in other regions (Fig. 6, Cx43).

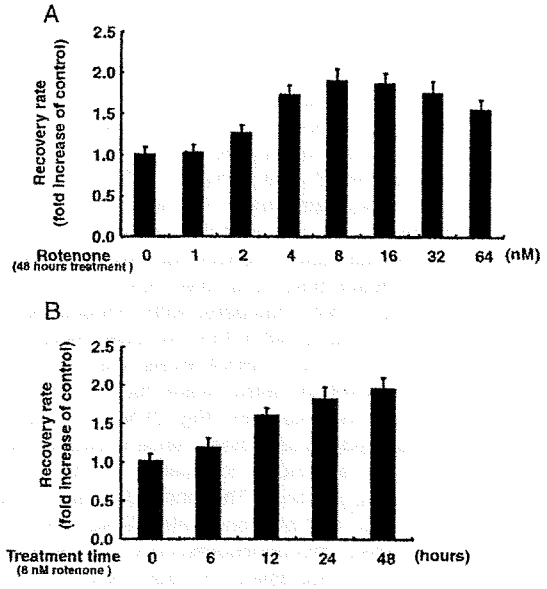

Fig. 3. Dose and time course analyses of the effect of rotenone on GJIC in cultured astrocytes. GJIC was assessed by FRAP, in terms of RR (fold increase of control cells). Results are means of at least three experiments. (A) Dose dependence (treatment for 48 h). (B) Time dependence in the case of 8 nM rotenone. Columns show fold increase in RR compared with untreated cells (at 48 h) or compared with cells treated with 8 nM rotenone at 0 h for A or B, respectively. $P_{trend}<0.001$ for A and B.

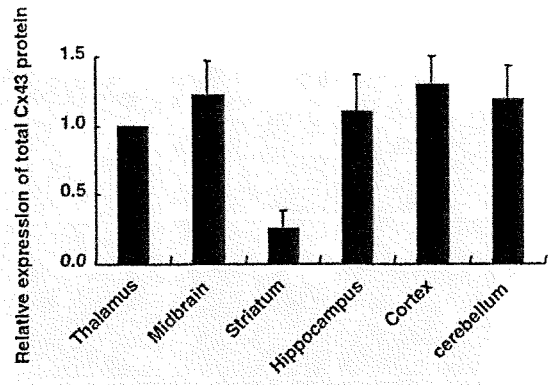

Fig. 4. Cx43 levels were compared between different brain regions by using identical membranes loaded with the homogenates obtained from the different regions. The graph depicts fold increase of total Cx43 expression relative to the control (thalamus). Values are mean±SE with $n=3$.

In addition, although astrocytes were denser in SNr and GP than in SNc and striatum, the numbers of astrocytes in nigrostriatal regions was unchanged with rotenone treatment (Fig. 6, GFAP).

DISCUSSION

Previous Cx43 electrophoresis studies had found a faster-migrating form that includes nonphosphorylated Cx43 (P_0) and at least two slower-migrating forms, commonly termed P_1 and P_2 (Crow et al., 1990; Musil et al., 1990). Pulse-chase analysis had indicated that the Cx43 isoforms progress from P_0 to P_1 to P_2 and that the P_2 isoform is associated with gap junctional structures (Musil and Goodenough, 1991). In our study, rotenone treatment induced an increase of total Cx43 protein in astrocytes, and the number of localized foci of total and phosphorylated Cx43 on the plasma membrane was increased. Furthermore, astrocyte GJIC was intensified with rotenone treatment. Therefore, since the increase of P_1 and P_2forms of Cx43 was proportional to the increase of total Cx43 protein levels, our findings indicate that phosphorylation of P_0 and P_1 was enhanced during the induction of total Cx43 protein by rotenone. Cowan et al. (2003) reported that Cx43 protein levels decreased in response to rotenone treatment, but their finding cannot be directly compared with ours, since they used vascular smooth muscle cells and a far higher concentration (10 μM) of rotenone.

On the other hand, since *Cx43* mRNA levels did not change, altered protein degradation may be involved in the rotenone-induced increase of Cx43 protein. Degradation of Cx43 is thought to be regulated by phosphorylation of P_0, or possibly P_1 and P_2 (Rivedal and Opsahl, 2001; Ruch et al., 2001; Qin et al., 2003). Phosphorylation is implicated in the regulation of GJIC at several stages of the connexin "life cycle," including trafficking, assembly/disassembly, and gating of gap junction channels (Lampe and Lau, 2004). Our *in vivo* experiment using rotenone-treated rats demonstrated for the first time that P_1 and P_2 forms of Cx43 are selectively induced in astrocytes of the basal ganglia regions, which contain DA neurons or their terminal areas, and that these elevated levels of Cx43 were sustained during rotenone treatment. This site-specific

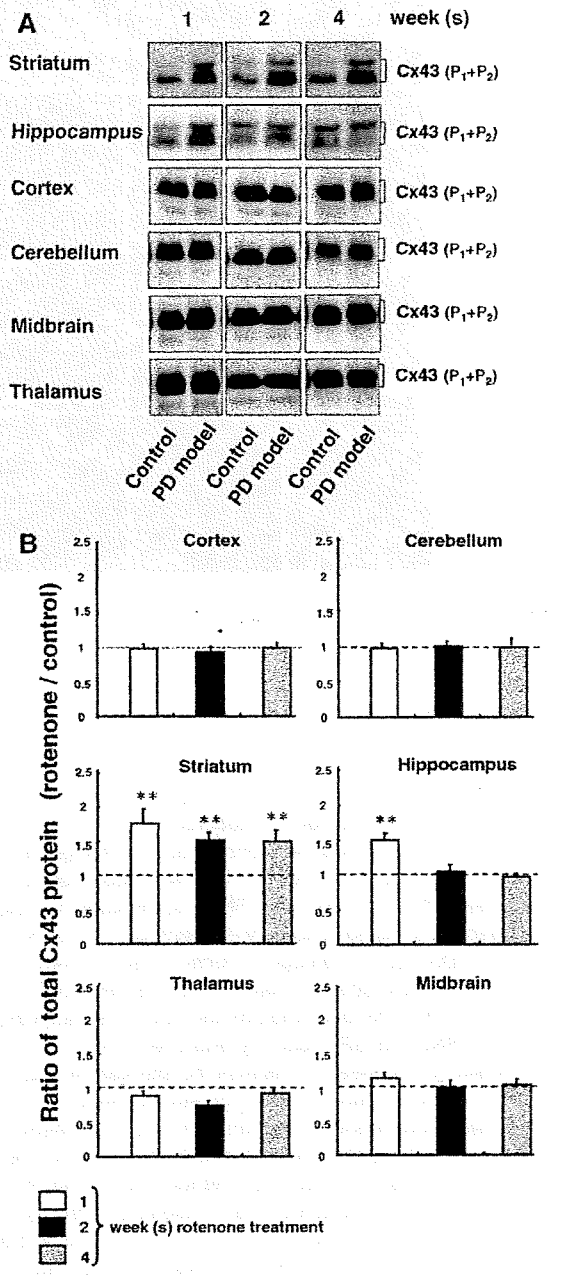

Fig. 5. Cx43 levels in the brain of rotenone-treated rats relative to that of Panacet (vehicle)-treated rats (control) at 1, 2, and 4 weeks. (A) Western blotting analysis of Cx43. (B) Column illustrates the quantifications of Cx43 levels obtained from three independent experiments by measuring the intensity of the Cx43 signal. Values are mean±SE with $n=6$. ** $P<0.05$ for the mean difference from the corresponding control group.

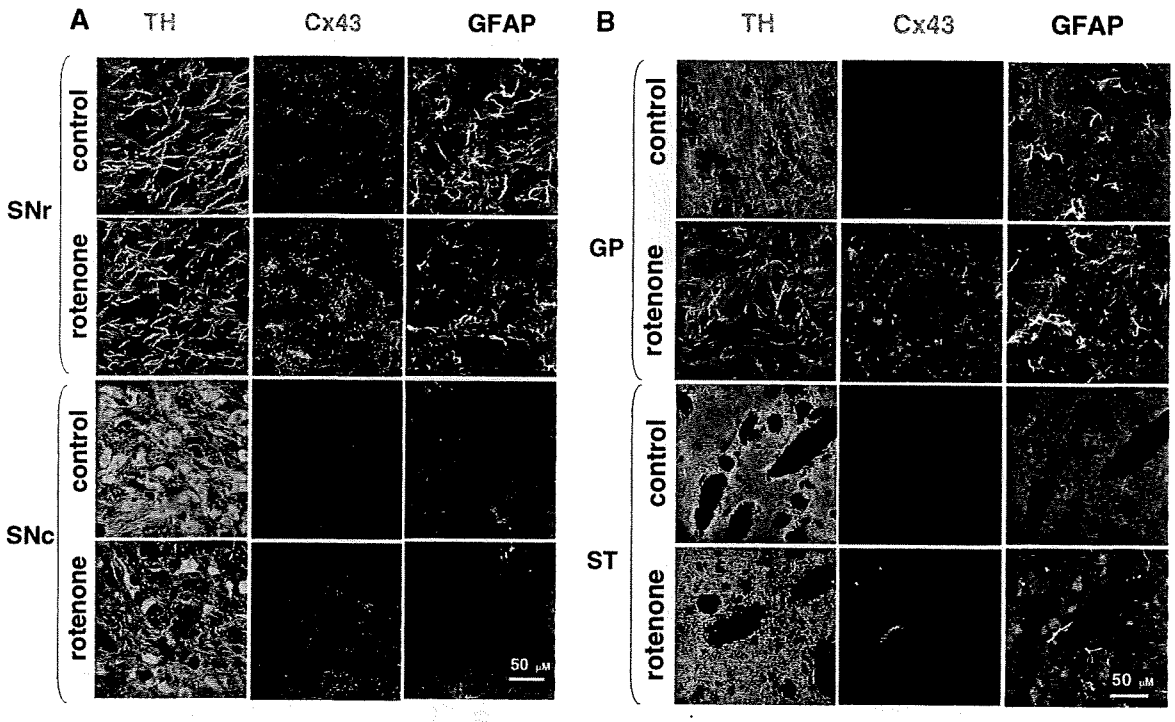

Fig. 6. Immunofluorescence staining of (A) SN and (B) ST obtained from Panacet- (vehicle) or rotenone-treated rat brain at 4 weeks. Triple labeling was used, with TH colored green, Cx43 colored red, and GFAP, an astrocyte marker, colored white. In (B) GP or ST indicates globus pallidus or striatum, respectively. Scale bars=50 μM.

susceptibility of astrocytes to Cx43 induction by rotenone could be of great importance, since the great heterogeneity of astrocytes among brain sites is a key to understanding PD pathology (Price et al., 1999; Amadio et al., 2007).

This study has obvious limitations, and some tasks for future investigation are mentioned below. Although induction of astrocyte Cx43 by rotenone was observed along with loss of DA neurons in the SNc and striatum, we failed to establish a relationship between increase of Cx43 and extent of DA neuron damage: induced levels of Cx43 were lower in SNc and striatum than in SNr and GP, though DA neurons in the SNc and striatum are more vulnerable than those in SNr and GP (Fearnley and Lees, 1991). Further study will be necessary to assess the site-specific vulnerability of DA neurons in the nigrostriatal area, and the potential involvement of mechanisms, such as inflammation, other than GJIC in the selective death of DA neurons. Induction of Parkinsonism by rotenone will need to be examined. For example, the inflammation that is thought to cause activation of astrocytes, which is in turn associated with upregulation of Cx43, may involve microglia (Retamal et al., 2007). In addition, Cx30 and Cx26 are both major gap junction proteins in astrocytes. We found that Cx26 expression was unaffected by rotenone *in vivo* and *in vitro* (data not shown), but it will also be necessary to examine changes in Cx30 in the future, perhaps with the use of Cx.-specific inhibitors or siRNA.

The central question is whether the elevation of astrocyte GJIC plays a part in causing the development of PD or whether it is merely a protective response to rotenone. Astrocytic syncytia in the normal CNS play important homeostatic roles in the spatial buffering of extracellular potassium ions and water (Jefferys, 1995; Naus et al., 1997; Wallraff et al., 2006), glutamate and other signaling molecules (Cornell-Bell et al., 1990; Hossain et al., 1994), and energy sources (Dienel and Cruz, 2003). On the other hand, abnormal synchronization of the oscillatory activity of neurons at multiple levels of the basal ganglia–cortical loop is thought to play a role in this synchronization in animal models and human PD. This suggests the possibility that enhancement of GJIC affects PD development (Yamawaki et al., 2008). To examine whether this is so, the effects of astrocyte GJIC inhibition on DA neurons in PD models needs to be investigated using an astrocyte-specific GJIC inhibitor; however, such an inhibitor is not yet available. Cx. knockout mice might be useful to investigate the role of gap junctions in PD models. Furthermore, it is of interest to know why the change of Cx43 occurred in the hippocampus. Our immunohistological analysis suggested that the number of astrocytes in striatum and hippocampus is higher than those in other brain regions. Therefore one possibility is that this difference in the density of astrocytes influences the induction of Cx43 protein by rotenone. Another possibility is that astrocytes in striatum and hip-

pocampus might have different characteristics from those in other areas (Price et al., 1999; Amadio et al., 2007).

Rufer et al. (1996) reported that immunoreactive Cx43 protein was increased in the striatum in a rat MPTP model, but they did not find evidence of increased functional coupling. They did not examine cultured astrocytes. The reason for the difference between their results and ours is unclear, but may be related to the differences between the rotenone and MPTP models. In summary, rotenone enhanced GJIC through induction of phosphorylated Cx43 as well as total Cx43 in astrocytes, and increased Cx43 in nigrostriatal astrocytes was also observed in rotenone-treated rats, accompanied with loss of DA neurons. Given the potential implications of our findings, the mechanisms linking enhanced astrocyte GJIC and DA neuron death urgently need to be examined.

Acknowledgments—The authors would like to thank Dr. Takashi Taniguchi and Dr. Yoshihisa Kitamura and Takashi Yanagida from Kyoto Pharmaceutical University, and Dr. Koichiro Ozawa and Dr. Toru Hosoi from Graduate School of Biomedical Sciences, Hiroshima University.

REFERENCES

Alam M, Schmidt WJ (2002) Rotenone destroys dopaminergic neurons and induces parkinsonian symptoms in rats. Behav Brain Res 136:317–324.

Amadio S, Montilli C, Picconi B, Calabresi P, Volonte C (2007) Mapping P2X and P2Y receptor proteins in striatum and substantia nigra: an immunohistological study. Purinergic Signal 3:389–398.

Anderson CM, Swanson RA (2000) Astrocyte glutamate transport: review of properties, regulation, and physiological functions. Glia 32:1–14.

Araki T, Kumagai T, Tanaka K, Matsubara M, Kato H, Itoyama Y, Imai Y (2001) Neuroprotective effect of riluzole in MPTP-treated mice. Brain Res 918:176–181.

Betarbet R, Sherer TB, MacKenzie G, Garcia-Osuna M, Panov AV, Greenamyre JT (2000) Chronic systemic pesticide exposure reproduces features of Parkinson's disease. Nat Neurosci 3:1301–1306.

Cardona AE, Pioro EP, Sasse ME, Kostenko V, Cardona SM, Dijkstra IM, Huang D, Kidd G, Dombrowski S, Dutta R, Lee JC, Cook DN, Jung S, Lira SA, Littman DR, Ransohoff RM (2006) Control of microglial neurotoxicity by the fractalkine receptor. Nat Neurosci 9:917–924.

Cornell-Bell AH, Finkbeiner SM, Cooper MS, Smith SJ (1990) Glutamate induces calcium waves in cultured astrocytes: long-range glial signaling. Science 247:470–473.

Cowan DB, Jones M, Garcia LM, Noria S, del Nido PJ, McGowan FX Jr (2003) Hypoxia and stretch regulate intercellular communication in vascular smooth muscle cells through reactive oxygen species formation. Arterioscler Thromb Vasc Biol 23:1754–1760.

Crow DS, Beyer EC, Paul DL, Kobe SS, Lau AF (1990) Phosphorylation of connexin43 Gap junction protein in uninfected and Rous sarcoma virus-transformed mammalian fibroblasts. Mol Cell Biol 10:1754–1763.

Dermietzel R, Gao Y, Scemes E, Vieira D, Urban M, Kremer M, Bennett MV, Spray DC (2000) Connexin 43 null mice reveal that astrocytes express multiple connexins. Brain Res Brain Res Rev 32:45–56.

Dienel GA, Cruz NF (2003) Neighborly interactions of metabolically-activated astrocytes in vivo. Neurochem Int 43:339–354.

Fearnley JM, Lees AJ (1991) Ageing and Parkinson's disease: substantia nigra regional selectivity. Brain 114(5):2283–2301.

Haupt C, Witte OW, Frahm C (2007) Upregulation of connexin 43 in the glial scar following photothrombotic ischemic injury. Mol Cell Neurosci 35:89–99.

Hayashi T, Matesic DF, Nomata K, Kang KS, Chang CC, Trosko JE (1997) Stimulation of cell proliferation and inhibition of gap junctional intercellular communication by linoleic acid. Cancer Lett 112:103–111.

Hosoi T, Okuma Y, Nomura Y (2000) Expression of leptin receptors and induction of IL-1beta transcript in glial cells. Biochem Biophys Res Commun 273:312–315.

Hossain MZ, Peeling J, Sutherland GR, Hertzberg EL, Nagy JI (1994) Ischemia-induced cellular redistribution of the astrocytic gap junctional protein connexin43 in rat brain. Brain Res 652:311–322.

Jefferys JG (1995) Nonsynaptic modulation of neuronal activity in the brain: electric currents and extracellular ions. Physiol Rev 75: 689–723.

Kielian T (2008) Glial connexins and gap junctions in CNS inflammation and disease. J Neurochem 106:1000–1016.

Lampe PD, Lau AF (2004) The effects of connexin phosphorylation on gap junctional communication. Int J Biochem Cell Biol 36:1171–1186.

McGeer PL, McGeer EG (2008) Glial reactions in Parkinson's disease. Mov Disord 23:474–483.

Meme W, Calvo CF, Froger N, Ezan P, Amigou E, Koulakoff A, Giaume C (2006) Proinflammatory cytokines released from microglia inhibit gap junctions in astrocytes: potentiation by beta-amyloid. FASEB J 20:494–496.

Musil LS, Cunningham BA, Edelman GM, Goodenough DA (1990) Differential phosphorylation of the Gap junction protein connexin43 in junctional communication-competent and -deficient cell lines. J Cell Biol 111:2077–2088.

Musil LS, Goodenough DA (1991) Biochemical analysis of connexin43 intracellular transport, phosphorylation, and assembly into gap junctional plaques. J Cell Biol 115:1357–1374.

Nagy JI, Li W, Hertzberg EL, Marotta CA (1996) Elevated connexin43 immunoreactivity at sites of amyloid plaques in Alzheimer's disease. Brain Res 717:173–178.

Nagy JI, Rash JE (2003) Astrocyte and oligodendrocyte connexins of the glial syncytium in relation to astrocyte anatomical domains and spatial buffering. Cell Commun Adhes 10:401–406.

Naus CC, Bechberger JF, Zhang Y, Venance L, Yamasaki H, Juneja SC, Kidder GM, Giaume C (1997) Altered gap junctional communication, intercellular signaling, and growth in cultured astrocytes deficient in connexin43. J Neurosci Res 49:528–540.

Obata T, Aomine M, Yamanaka Y (2000) Potassium chloride depolarization enhances MPP+-induced hydroxyl radical generation in the rat striatum. Brain Res 852:488–491.

Ogawa T, Hayashi T, Tokunou M, Nakachi K, Trosko JE, Chang CC, Yorioka N (2005) Suberoylanilide hydroxamic acid enhances gap junctional intercellular communication via acetylation of histone containing connexin 43 gene locus. Cancer Res 65:9771–9778.

Price CJ, Kim P, Raymond LA (1999) D1 dopamine receptor-induced cyclic AMP-dependent protein kinase phosphorylation and potentiation of striatal glutamate receptors. J Neurochem 73:2441–2446.

Qin H, Shao Q, Igdoura SA, Alaoui-Jamali MA, Laird DW (2003) Lysosomal and proteasomal degradation play distinct roles in the life cycle of Cx43 in gap junctional intercellular communication-deficient and -competent breast tumor cells. J Biol Chem 278: 30005–30014.

Ransom B, Behar T, Nedergaard M (2003) New roles for astrocytes (stars at last). Trends Neurosci 26:520–522.

Retamal MA, Froger N, Palacios-Prado N, Ezan P, Saez PJ, Saez JC, Giaume C (2007) Cx43 hemichannels and gap junction channels in astrocytes are regulated oppositely by proinflammatory cytokines released from activated microglia. J Neurosci 27:13781–13792.

Rivedal E, Opsahl H (2001) Role of PKC and MAP kinase in EGF- and TPA-induced connexin43 phosphorylation and inhibition of gap

junction intercellular communication in rat liver epithelial cells. Carcinogenesis 22:1543–1550.

Rouach N, Glowinski J, Giaume C (2000) Activity-dependent neuronal control of gap-junctional communication in astrocytes. J Cell Biol 149:1513–1526.

Ruch RJ, Trosko JE, Madhukar BV (2001) Inhibition of connexin43 gap junctional intercellular communication by TPA requires ERK activation. J Cell Biochem 83:163–169.

Rufer M, Wirth SB, Hofer A, Dermietzel R, Pastor A, Kettenmann H, Unsicker K (1996) Regulation of connexin 43, GFAP, and FGF-2 is not accompanied by changes in astroglial coupling in MPTP-lesioned, FGF-2-treated parkinsonian mice. J Neurosci Res 46:606–617.

Trosko JE, Chang CC, Wilson MR, Upham B, Hayashi T, Wade M (2000) Gap junctions and the regulation of cellular functions of stem cells during development and differentiation. Methods 20:245–264.

Vis JC, Nicholson LF, Faull RL, Evans WH, Severs NJ, Green CR (1998) Connexin expression in Huntington's diseased human brain. Cell Biol Int 22:837–847.

Wade MH, Trosko JE, Schindler M (1986) A fluorescence photobleaching assay of gap junction-mediated communication between human cells. Science 232:525–528.

Wallraff A, Kohling R, Heinemann U, Theis M, Willecke K, Steinhauser C (2006) The impact of astrocytic gap junctional coupling on potassium buffering in the hippocampus. J Neurosci 26: 5438–5447.

Yamawaki N, Stanford IM, Hall SD, Woodhall GL (2008) Pharmacologically induced and stimulus evoked rhythmic neuronal oscillatory activity in the primary motor cortex in vitro. Neuroscience 151:386–395.

APPENDIX

Supplementary data

Supplementary data associated with this article can be found, in the online version, at doi: 10.1016/j.neuroscience.2009.01.080.

(Accepted 31 January 2009)
(Available online 13 February 2009)

Int. J. Radiat. Biol., Vol. 86, No. 1, January 2010, pp. 56–62

Memory CD4 T-cell subsets discriminated by CD43 expression level in A-bomb survivors

SEISHI KYOIZUMI[1,3], MIKA YAMAOKA[1], YOSHIKO KUBO[1], KANYA HAMASAKI[1], TOMONORI HAYASHI[1], KEI NAKACHI[1], FUMIYOSHI KASAGI[2], & YOICHIRO KUSUNOKI[1]

Departments of [1]Radiobiology/Molecular Epidemiology and [2]Epidemiology, Radiation Effects Research Foundation, and [3]Department of Nutritional Sciences, Faculty of Human Ecology, Yasuda Women's University, Hiroshima, Japan

(Received 27 October 2008; Revised 18 May 2009; Accepted 20 July 2009)

Abstract

Purpose: Our previous study showed that radiation exposure reduced the diversity of repertoires of memory thymus-derived cells (T cells) with cluster of differentiation (CD)- 4 among atomic-bomb (A-bomb) survivors. To evaluate the maintenance of T-cell memory within A-bomb survivors 60 years after radiation exposure, we examined functionally distinct memory CD4 T-cell subsets in the peripheral blood lymphocytes of the survivors.

Methods: Three functionally different subsets of memory CD4 T cells were identified by differential CD43 expression levels and measured using flow cytometry. These subsets consist of functionally mature memory cells, cells weakly responsive to antigenic stimulation, and those cells functionally anergic and prone to spontaneous apoptosis.

Results: The percentages of these subsets within the peripheral blood CD4 T-cell pool all significantly increased with age. Percentages of functionally weak and anergic subsets were also found to increase with radiation dose, fitting to a log linear model. Within the memory CD4 T-cell pool, however, there was an inverse association between radiation dose and the percentage of functionally mature memory cells.

Conclusion: These results suggest that the steady state of T cell memory, which is regulated by cell activation and/or cell survival processes in subsets, may have been perturbed by prior radiation exposure among A-bomb survivors.

Keywords: *A-bomb, CD4, immunological memory, CD43, flow cytometry, T cell*

Introduction

In humans, immunological memory resides in and is controlled by long-lived lymphocytes, with immunologic memory being maintained at an appropriate level by a constant proliferation of memory thymus-derived cells (T cells) (Dutton et al. 1998). Once subjected to antigenic stimulation, memory T cells tend to divide repeatedly, thus giving rise to greatly expanded clonal populations which may persist for very long periods of time (Maini et al. 1999). Clonally expanded T-cell populations are frequently observed not only in healthy aged persons (Posnett et al. 1994, Fitzgerald et al. 1995, Wack et al. 1998) but also in virally-infected individuals (Eiraku et al. 1998, Silins et al. 1998) and in patients with autoimmune diseases of various types (Fitzgerald et al. 1995, Musette et al. 1996, Waase et al. 1996).

In general, the peripheral blood pool of memory T cells with cluster of differentiation (CD)- 4 appear not to have been significantly affected by radiation exposure among atomic-bomb (A-bomb) survivors. However, there are significant dose-dependent deficits in the naïve T-cell pools (Kusunoki et al. 1998, 2002, Yamaoka et al. 2004). Further, clonal populations originating from peripheral T cells have been identified in blood samples from some of the A-bomb survivors primarily by tracking specific T-cell receptor (TCR) genes and/or chromosome aberrations in memory T-cell populations (Kusunoki et al. 1993, Nakano et al. 2004). In this regard, we have recently reported that the extent of deviation in the TCR repertoire of memory CD4 T cells significantly increased as the intensity of radiation exposure increased (Kusunoki et al. 2003). It seems reasonable, therefore, to assume that A-bomb radiation

Correspondence: Yoichiro Kusunoki, PhD, Department of Radiobiology/Molecular Epidemiology, Radiation Effects Research Foundation, 5-2 Hijiyama Park, Minami-ku, Hiroshima, 732-0815 Japan. Tel: +81 82261 3131. Fax: +81 82261 3170. E-mail: ykusunok@rerf.or.jp

ISSN 0955-3002 print/ISSN 1362-3095 online
DOI: 10.3109/09553000903272641

induced the expansion or shrinkage of particular memory T-cell clones, concomitant with a reduced capacity to maintain fully diverse repertoires of helper T-cell memory.

Previously, we have reported that human memory CD4 T cells can be discriminated into three functionally different subsets (M1, M2, and M3) using the human stem cell-associated (HSCA)- 2 monoclonal antibody (mAb) that recognises a sialic acid-dependent epitope on the low molecular mass (~115 kDa) glycoform of CD43 (Ohara et al. 2002, Kyoizumi et al. 2004). The M1 subset consists of functionally mature cells whose CD43 expression is relatively high. The M2 subset expresses moderate levels of CD43, and responds weakly to TCR-mediated stimuli. The M3 subset exhibits relatively low levels of CD43 and is anergic to TCR-mediated stimuli, and prone to spontaneous apoptosis.

In this study, we evaluated the extent to which T-cell memory function is retained in A-bomb survivors by examining the relationships between these memory CD4 T-cell subsets, ageing, and radiation exposure.

Materials and methods

Blood donors

An A-bomb survivor cohort was randomly selected from a group of Hiroshima participants in the Adult Health Study (AHS) at the Radiation Effects Research Foundation (RERF) (Kodama et al. 1996).

For the present study, blood samples of 1132 survivors were obtained, with informed consent, from survivors who participated in the AHS between 2004 and 2008. This study protocol has been approved by the Human Investigation Committee of RERF. We excluded 216 subjects (19% in total subjects) who had been diagnosed with cancer from the current study. Cancer prevalence by dose category was 16% at <0.005 Gy, 21% at 0.005–0.5 Gy, 30% at 0.5–1.0 Gy, and 35% at ≥1.0 Gy, and tended to be higher in survivors exposed to higher doses, in accord with a recent observation in the AHS population (Kyoizumi et al. 2005). The age, gender and radiation dose of the remaining 916 survivors whose lymphocyte samples were subjected to data analysis in our study are listed in Table I. Radiation doses are based on the Dosimetry System 2002 (DS02) estimates (Cullings et al. 2006).

Table I. Age, gender, and radiation dose distribution of study population.

Dose (Gy)	Age (yrs)[b] category						
	60–69 yrs		70–79 yrs		≥80 yrs		
	Male	Female	Male	Female	Male	Female	Total
<0.005[a]	27	25	58	84	17	94	305
0.005–0.5	13	33	54	66	22	107	295
0.5–1.0	19	18	20	33	9	49	148
1.0–4.0	28	25	28	35	14	38	168
Total	87	101	160	218	62	288	916

[a]Individuals in this dose category were exposed at distances in excess of 3 km from the hypocenter, and hence received doses that are substantially equivalent to zero. [b]Age at the time of the examinations that were conducted between 2004 and 2008.

Flow cytometry

Mononuclear cell fractions separated by the Ficoll-Hypaque gradient technique were analysed by three-colour flow cytometry using a FACScan flow cytometer (BD Biosciences, San Jose, CA, USA). Fluorescein isothiocyanate (FITC)-labelled HSCA-2 mAb was prepared as described previously (Kyoizumi et al. 2004). PerCP-labelled CD4 mAb and phycoerythrin (PE)-labelled CD45-related O (CD45RO) mAb were purchased from BD-PharMingen (San Diego, CA, USA) and Caltag Laboratories (Burlingame, CA, USA), respectively. Three different memory CD4 subsets were defined: $CD45RO^+$ cells that expressed higher (M1), intermediate (M2), and lower (M3) levels of CD43. For each donor specimen, the window for the M2 subset was set in a range where CD43 level was from ½- to 2-fold of the mean CD43 intensity for $CD45RO^-$ cells, and the windows for the M1 and M3 subsets were set just to the right and left sides of the M2 window, respectively (Figure 1). Note that this method of memory CD4 T-cell subset discrimination was established in a previous study (Ohara et al. 2002) in which functional and phenotypical differences among these subsets were characterised, using a gating procedure (i.e., that involved internal standardisation of fluorescence intensities) that avoided the effects of inter-experimental variability. The percentage of cells in the range of each subset was obtained in a total CD4 T-cell population.

Data analysis

Associations of the percentage of each memory CD4 T-cell subpopulation (*percentage*) with age at time of examination (*age*), gender (*gender*), and radiation dose (*dose*) were analysed using a multiple regression model (Armitage et al. 2002). The method assumed that the percentage of each T-cell subpopulation related to each explanatory variable in a log linear manner:

$$\log(percentage = \alpha + \beta_1(age - 70) + \beta_2 gender + \beta_3 does,$$

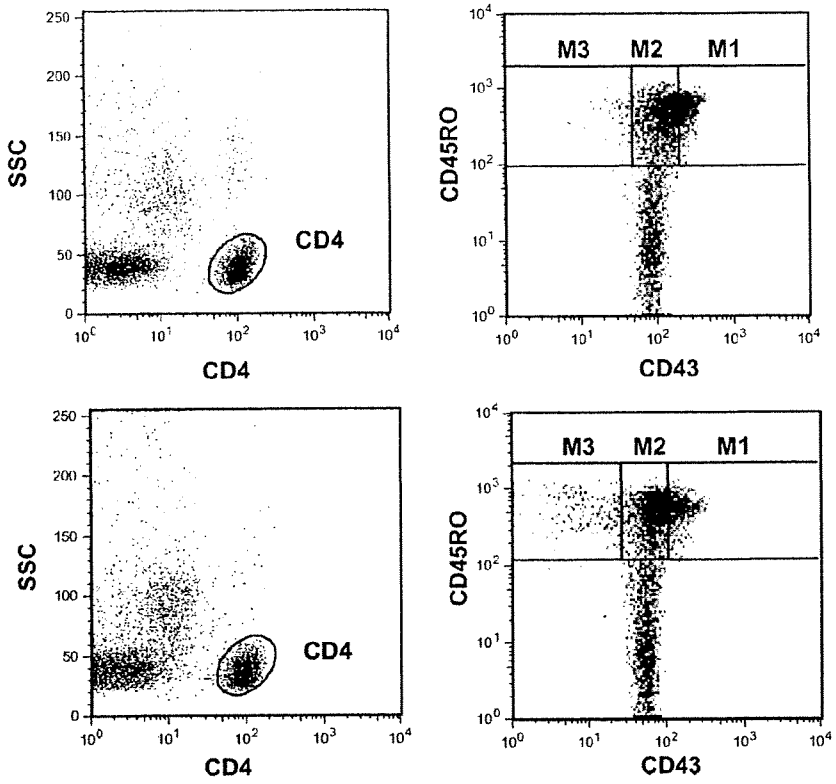

Figure 1. Flow cytometry patterns of CD4 T cells in the peripheral blood of 79-year-old females whose estimated radiation doses were zero (upper) and 0.525 Gy (lower). Peripheral blood mononuclear cells (about 2×10^5) were stained with FITC-labelled CD43 (HSCA-2) mAb, PE-labelled CD45RO mAb, and PerCP-labelled CD4 mAb. CD4 T cells were gated based on side light scattering (SSC) and CD4 intensity (left) and analysed for their expression of CD43 and CD45RO (right). Percentages of memory CD4 T-cell subsets in a total CD4 T-cell population of the unexposed were 24.1 for M1, 30.4 for M2, and 4.8 for M3, and those of the exposed were 17.2 for M1, 35.1 for M2, and 10.6 for M3.

where *gender* is an indicator of female sex, i.e., *gender* = 0 for male and *gender* = 1 for female, and *dose* is radiation dose in grays. The α is a constant term, and $\beta_1, \beta_2, and \beta_3$ are regression coefficients for variables to be estimated. The age term was subtracted by 70 years so that α corresponds to log-transformed percentage of CD4 T-cell subset, i.e., the subset percentage is calculated to be e^{α} (=exponential [α]), for non-irradiated males at 70 years of age. The % change of subset percentage was estimated to be $100(e^{10\beta_1}-1)$ per 10 years increment of age, and $100(e^{\beta_3}-1)$ per 1 Gy radiation dose. This regression analysis in the log linear manner was applied to evaluate the association of the percentage of memory subset within the CD4 T-cell population or CD45RO-positive memory CD4 T-cell population with age or radiation dose.

Results

Figure 1 shows the flow cytometry patterns of memory CD4 T-cell subsets within blood lymphocyte specimens of two age-matched women whose estimated exposure doses were zero and 0.525 Gy, respectively. Crude mean of percentage of each memory T-cell subset within the CD4 T-cell population was shown by age category and by dose category in Tables II and III, respectively. Table IV shows the association of the percentage of each memory T-cell subset with age and radiation dose, in terms of a multiple regression model. The percentage of memory cells (identified and enumerated by CD45RO-positivity) within the CD4 T-cell population appeared to significantly increase with age ($p < 0.0001$), and also with radiation dose ($p = 0.0060$). There was no difference in the percentage of CD45RO-positive memory cells between males and females (data not shown). As for memory T-cell subsets (M1, M2, and M3), the percentage of each subset in the CD4 T-cell population appeared to significantly increase with age ($p < 0.0001$); but again, these percentages did not differ between males and females (data not shown). The percentages of M2 ($p = 0.0001$) and M3 ($p = 0.0096$) subsets were found to significantly increase with radiation dose.

Table II. Crude means of the percentages of memory subsets in the CD4 T-cell population by age category.

	Age category		
	60–69 yrs	70–79 yrs	≥80 yrs
Subset	Mean 65.5 yrs	75.7 yrs	84.8 yrs
CD45 RO (total memory)	48.8 (1.10)[a]	52.2 (0.85)	58.1 (0.87)
M1 (mature, fully competent)	17.3 (0.62)	18.7 (0.49)	22.4 (0.56)
M2 (immature, poorly competent)	26.1 (0.57)	27.4 (0.43)	29.3 (0.45)
M3 (death prone, anergic)	5.3 (0.14)	6.1 (0.17)	6.4 (0.14)

[a]Standard error in parentheses.

Table III. Crude means of the percentages of memory subsets in the CD4 T-cell population by dose category.

	Radiation dose category			
	<0.005 Gy	0.005–0.5 Gy	0.5–1.0 Gy	1.0–4.0 Gy
Subset	Mean 0.0 Gy	0.20 Gy	0.75 Gy	1.74 Gy
CD45 RO	53.3 (0.93)[a]	53.1 (0.99)	55.0 (1.49)	54.6 (1.13)
M1	19.8 (0.57)	20.1 (0.57)	20.0 (0.88)	19.3 (0.72)
M2	27.4 (0.47)	27.2 (0.51)	29.0 (0.75)	29.0 (0.57)
M3	6.1 (0.18)	5.8 (0.14)	6.0 (0.21)	6.3 (0.20)

[a]Standard error in parentheses.

Table IV. Association of the percentages of memory subsets in the CD4 T-cell population with age or dose (multiple regression analysis)[a].

	% change of subset percentage per unit	
Subset	Age (10 years)[b]	Dose (1 Gy)[c]
CD45RO	10.8	4.3
	(8.0, 13.5)[d]	(1.3, 7.3)
	$p < 0.0001$	$p = 0.0060$
M1	14.6	1.3
	(10.1, 19.1)	(−3.7, 6.2)
	$p < 0.0001$	$p = 0.61$
M2	7.3	5.8
	(4.7, 10.0)	(2.9, 8.7)
	$p < 0.0001$	$p = 0.0001$
M3	10.6	4.9
	(7.2, 13.9)	(1.2, 8.6)
	$p < 0.0001$	$p = 0.0096$

[a]Representative memory subset percentage (95% confidence interval) for non-irradiated males at 70 years of age was calculated to be 15.3 (13.9, 16.7) for M1, 24.8 (23.6, 26.0) for M2, and 5.1 (3.9, 6.4) for M3. Note that there was no significant difference in the percentage of total CD45RO-positive memory cells and that of each memory T-cell subset between males and females. [b]Effects of age were estimated for 10 years. [c]Effects of radiation dose were estimated for 1 Gy. [d]95% confidence interval.

These radiation dose-related changes of memory T-cell subsets observed within the CD4 T-cell population may also involve comparable changes within memory subsets of the CD45RO-positive CD4 T-cell population (Table V). The percentages of M1 and M2 subsets in the memory CD4 T-cell population appeared to significantly increase and decrease with age ($p = 0.0085$ and $p < 0.0001$), respectively. In association with radiation dose, there was a statistically significant decrease in the percentage of M1 subset within the CD45RO-positive memory CD4 T cell population ($p = 0.039$). The ratio of the M1 subset to the combined M2 and M3 subsets also significantly decreased with radiation dose ($p = 0.043$), in contrast to a significant increase in this ratio with age ($p = 0.0030$).

Discussion

Our previous study (Ohara et al. 2002) has clearly shown functional differences among M1, M2, and M3 memory T-cell subsets: Cells in the M1 subset have greater capacity to respond to recall antigens (such as tuberculosis purified protein derivative and tetanus toxoid) and to secrete interferon-γ and IL-4 than cells in either of the other subsets; the M2 subset is comprised of memory-type cells that are less mature than cells of the M1 subset, in terms of not only their memory cell function (i.e., recall antigen reactivity and cytokine-producing ability), but also in terms of their chromosomes' telomere length (longer telomeres); and the M3 subset, in contrast to the M2 subset, consists of cells that are anergic to TCR-mediated stimuli and prone to apoptosis. Therefore, an increase in the proportion of these functionally less competent T-cell subsets (i.e., M2 and M3) may

Table V. Comparable changes of memory subsets within CD45RO-positive memory CD4 T-cell population with age or dose (multiple regression analysis).

	% change of subset percentage per unit	
Subset	Age (10 years)[a]	Dose (1 Gy)[b]
M1	3.5	−3.0
	(0.9, 6.1)[c]	(−5.8, −0.2)
	$p = 0.0085$	$p = 0.039$
M2	−3.2	1.5
	(−4.6, −1.8)	(−0.6, 3.0)
	$p < 0.0001$	$p = 0.059$
M3	−0.2	0.6
	(−3.4, 3.0)	(−2.9, 4.1)
	$p = 0.91$	$p = 0.73$
Ratio [M1/(M2 + M3)]	6.1	−4.5
	(2.1, 9.0)	(−8.8, −0.1)
	$p = 0.0030$	$p = 0.043$

[a]Effects of age were estimated for 10 years. [b]Effects of radiation dose were estimated for 1 Gy. [c]95% confidence interval.

not be beneficial to the individual in terms of immunological memory to previously encountered foreign antigens. Such preferential expansion of M2 and M3 subsets may also imply an insufficient maturation of antigen-primed CD4 T cells to the fully memory-competent M1 subset within the individuals' immune system. A hypothesis on memory CD4 T-cell differentiation pathways is depicted in Figure 2. After antigen exposure, naive T cells may undergo repeated cycles of cell division and transformation into the premature memory stage M2 cells. The conversion of M2 cells into the fully functioning mature memory stage M1 cells also requires population doublings following antigen exposure. Replication of M1 cells in response to recall antigens is largely responsible for the maintenance of memory functions. M3 cells, by contrast, are likely to be cells that are approaching senescence, and may arise from fully mature M1 cells that have lost survival signals such as cytokine signalling. We can also suspect that premature M2 cells are directly transformed into death-prone M3 cells. Such putative differentiation pathways may be controlled by interaction of memory T cells with antigen-presenting cells and environmental cytokine conditions. Such circumstances of memory T cells are very important to properly maintain immunological memory. In the CD4 T-cell systems of A-bomb survivors, there are at least two possibilities that the differentiation from M2 to M1 cells may be insufficient, and that cell transit from M2 and M1 subsets to apoptotic-prone M3 populations may be enhanced. Effects of radiation on cellular and molecular mechanisms controlling the memory T-cell differentiation pathways remain to be investigated. Taken together, our results suggest that function and maintenance of helper T-cell memory in the immune system of A-bomb survivors might have been compromised, after A-bomb irradiation.

Our previous study has shown that proliferative responsiveness of memory CD4 T cells to recall antigens can be enhanced by triggering cell-surface CD43 molecules with HSCA-2 mAb in vitro (Kyoizumi et al. 2004). That suggests that CD43 molecules play a part in certain of the cell signalling events involved in memory T-cell activation. Further, it is likely that CD43 and CD28 mAbs act synergistically to stimulate CD4 T-cell response to TCR cross-linking in vitro, indicating the co-stimulatory function of CD43 in TCR-mediated activation processes (Kyoizumi et al. 2004). It has also been suggested in the mouse immune system that the up-regulation of CD43 expression can have a negative effect on activation-induced cell death of T cells (He and Bevan 1999). A recent study has indicated that CD43 molecules induce a signalling cascade that prolongs the duration of TCR signal-mediated cell proliferation and cytokine secretion,

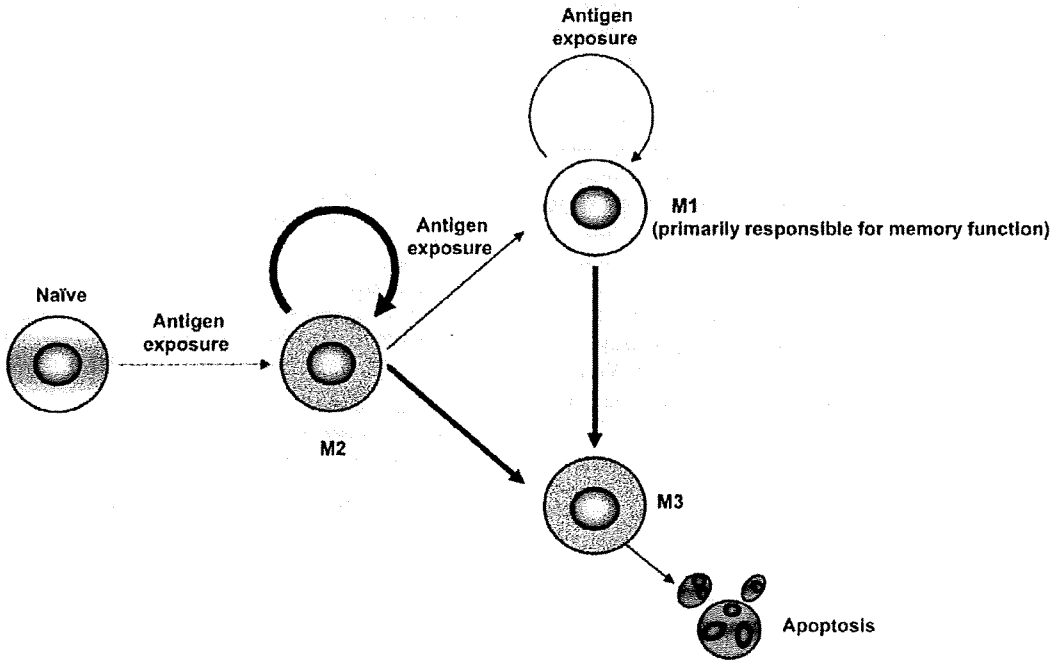

Figure 2. Hypothesised memory CD4 T-cell differentiation pathways for A-bomb survivors. Preferential pathways in the survivors' immune systems are drawn with bold lines.

but that prevents TCR signal-mediated anergy (Fierro et al. 2006). Thus, evidence is accumulating that there are positive effects of CD43-mediated signalling on activation and survival of memory T cells. By contrast, studies that have employed gene disruption techniques have shown that CD43 has either a negative regulatory role (Thurman et al. 1998, Tong et al. 2004), or possibly, plays no significant role in T-cell activation (Carlow et al. 2001). Although the precise mechanism of CD43-dependent regulation of T-cell activation remains to be determined, we have clearly demonstrated that CD43 expression is positively correlated with antigen responsiveness of memory CD4 T cells (Ohara et al. 2002). It is highly likely that the preferential increase in select memory subsets that express lower levels of CD43 (M2 and M3) may be associated with attenuated immune responses to specific pathogens. Levels of immunoglobulin G and A to *Chlamydia pneumoniae* have recently been found to decrease significantly with radiation dose among A-bomb survivors (Hakoda et al. 2006). It would be intriguing to study associations between antigen-specific responses to such ubiquitous pathogens and composition of memory T-cell subsets as defined by the relative level of CD43 expression among A-bomb survivors.

The individual's ability to properly maintain T-cell memory is known to decline with age (Goronzy and Weyand 2005, Weng 2006). This ageing-related immune attenuation is thought to be associated with: (i) The reduction in the size of naïve T-cell pool due to reduced production of new T cells within the involuted thymus, and subsequent, but infrequent entry of antigen-primed cells into the memory T-cell pool, and (ii) divergent antigen recognition repertoire of the memory T-cell pool due to the expansion or shrinkage of functionally incompetent memory T-cell populations (Goronzy and Weyand 2005, Weng 2006). Our previous observations of the immune system of A-bomb survivors are consistent with these typical features that relate to immunological ageing. In this regard, the proportion of naïve CD4 T cells was shown to decrease slightly, but significantly, with radiation dose (Kusunoki et al. 1998, 2002, Yamaoka et al. 2004). Also, the extent to which the TCR repertoire deviated from normal in memory CD4 T cells significantly increased with radiation dose in aged survivors (Kusunoki et al. 2003). An age-dependent increase in the percentage of M1 subset within the memory CD4 T-cell population may reflect the frequent expansion of functional memory T-cell populations in aged individuals. As far as we have examined for several individuals of the present study subjects, clonally expanded populations are largely distributed in M1 subset (Kyoizumi, manuscript in preparation), suggesting that, in aged individuals, only a small population of M1 subset may contribute to recall antigen responses in vivo. The observations in the present study can also be interpreted as an attenuation of helper T-cell memory possibly resulting from radiation-induced perturbation of T-cell homeostasis in A-bomb survivors.

Acknowledgements

The authors thank Dr Thomas M. Seed and Dr Evan B. Douple for careful reading of this manuscript. We are also grateful to Mika Yonezawa and Yoko Takemoto for their assistance with the manuscript preparation. The Radiation Effects Research Foundation (RERF), Hiroshima and Nagasaki, is a private non-profit foundation funded by the Japanese Ministry of Health, Labour and Welfare (MHLW) and the United States Department of Energy (DOE), the latter in part through the National Academy of Sciences. This publication was based on RERF Research Protocol RP 4-02 and supported in part by Grants-in-Aid for Scientific Research from Japan's Ministry of Education, Culture, Sports, Science, and Technology and MHLW.

Declaration of interest: The authors report no conflicts of interest. The authors alone are responsible for the content and writing of the paper.

References

Armitage G, Berry G, Matthews JNS. 2002. Statistical methods in medical research. Oxford: Blackwell Science.

Carlow DA, Corbel SY, Ziltener HJ. 2001. Absence of CD43 fails to alter T cell development and responsiveness. The Journal of Immunology 166:256–261.

Cullings HM, Fujita S, Funamoto S, Grant EJ, Kerr GD, Preston DL. 2006. Dose estimation for atomic bomb survivor studies: Its evolution and present status Radiation Research 166:219–254.

Dutton RW, Bradley LM, Swain SL. 1998. T cell memory. Annual Review of Immunology 16:201–223.

Eiraku N, Hingorani R, Ijichi S, Machigashira K, Gregersen PK, Monteiro J, Usuku K, Yashiki S, Sonoda S, Hall WW. 1998. Clonal expansion within $CD4^+$ and $CD8^+$ T cell subsets in human T lymphotropic virus type I-infected individuals. The Journal of Immunology 161:6674–6680.

Fierro NA, Pedraza-Alva G, Rosenstein Y. 2006. TCR-dependent cell response is modulated by the timing of CD43 engagement. The Journal of Immunology 176:7346–7353.

Fitzgerald JE, Ricalton NS, Meyer AC, West SG, Kaplan H, Behrendt C, Kotzin BL. 1995. Analysis of clonal $CD8^+$ T cell expansions in normal individuals and patients with rheumatoid arthritis. The Journal of Immunology 154:3538–3547.

Goronzy JJ, Weyand CM. 2005. T cell development and receptor diversity during aging. Current Opinion in Immunology 17:468–475.

Hakoda M, Kasagi F, Kusunoki Y, Matsuura S, Hayashi T, Kyoizumi S, Akahoshi M, Suzuki G, Kodama K, Fujiwara S. 2006. Levels of antibodies to microorganisms implicated in

atherosclerosis and of C-reactive protein among atomic bomb survivors. Radiation Research 166:360–366.

He YW, Bevan MJ. 1999. High level expression of CD43 inhibits T cell receptor/CD3-mediated apoptosis. The Journal of Experimental Medicine 190:1903–1908.

Kodama K, Mabuchi K, Shigematsu I. 1996. A long-term cohort study of the atomic-bomb survivors. Journal of Epidemiology 6(Suppl.):S95–105.

Kusunoki Y, Hirai Y, Hayashi T, Kyoizumi S, Takahashi K, Morishita Y, Kodama Y, Akiyama M. 1993. Frequent occurrence of in vivo clonal expansion of CD4 CD8 T cells bearing T cell receptor $\alpha\beta$ chains in adult humans. European Journal of Immunology 23:2735–2739.

Kusunoki Y, Kyoizumi S, Hirai Y, Suzuki T, Nakashima E, Kodama K, Seyama T. 1998. Flow cytometry measurements of subsets of T, B and NK cells in peripheral blood lymphocytes of atomic bomb survivors. Radiation Research 150:227–236.

Kusunoki Y, Yamaoka M, Kasagi F, Hayashi T, Koyama K, Kodama K, MacPhee DG, Kyoizumi S. 2002. T cells of atomic bomb survivors respond poorly to stimulation by *Staphylococcus aureus* toxins in vitro: Does this stem from their peripheral lymphocyte populations having a diminished naive CD4 T-cell content? Radiation Research 158:715–724.

Kusunoki Y, Yamaoka M, Kasagi F, Hayashi T, MacPhee DG, Kyoizumi S. 2003. Long-lasting changes in the T-cell receptor V beta repertoires of CD4 memory T-cell populations in the peripheral blood of radiation-exposed people. British Journal of Haematology 122:975–984.

Kyoizumi S, Kusunoki Y, Hayashi T, Hakoda M, Cologne JB, Nakachi K. 2005. Individual variation of somatic gene mutability in relation to cancer susceptibility: Prospective study on erythrocyte glycophorin A gene mutations of atomic bomb survivors. Cancer Research 65:5462–5469.

Kyoizumi S, Ohara T, Kusunoki Y, Hayashi T, Koyama K, Tsuyama N. 2004. Expression characteristics and stimulatory functions of CD43 in human $CD4^+$ memory T cells: Analysis using a monoclonal antibody to CD43 that has a novel lineage specificity. The Journal of Immunology 172:7246–7253.

Maini MK, Casorati G, Dellabona P, Wack A, Beverley PC. 1999. T-cell clonality in immune responses. Immunology Today 20:262–266.

Musette P, Bequet D, Delarbre C, Gachelin G, Kourilsky P, Dormont D. 1996. Expansion of a recurrent V beta 5.3^+ T-cell population in newly diagnosed and untreated HLA-DR2 multiple sclerosis patients. Proceedings of the National Academy of Sciences of the USA 93:12461–12466.

Nakano M, Kodama Y, Ohtaki K, Itoh M, Awa AA, Cologne J, Kusunoki Y, Nakamura N. 2004. Estimating the number of hematopoietic or lymphoid stem cells giving rise to clonal chromosome aberrations in blood T lymphocytes. Radiation Research. 161:273–281.

Ohara T, Koyama K, Kusunoki Y, Hayashi T, Tsuyama N, Kubo Y, Kyoizumi S. 2002. Memory functions and death proneness in three $CD4^+CD45RO^-$ human T cell subsets. The Journal of Immunology 169:39–48.

Posnett DN, Sinha R, Kabak S, Russo C. 1994. Clonal populations of T cells in normal elderly humans: The T cell equivalent to 'benign monoclonal gammapathy'. The Journal of Experimental Medicine 179:609–618.

Silins SL, Cross SM, Krauer KG, Moss DJ, Schmidt CW, Misko IS. 1998. A functional link for major TCR expansions in healthy adults caused by persistent Epstein-Barr virus infection. The Journal of Clinical Investigation 102:1551–1558.

Thurman EC, Walker J, Jayaraman S, Manjunath N, Ardman B, Green JM. 1998. Regulation of in vitro and in vivo T cell activation by CD43. International Immunology 10:691–701.

Waase I, Kayser C, Carlson PJ, Goronzy JJ, Weyand CM. 1996. Oligoclonal T cell proliferation in patients with rheumatoid arthritis and their unaffected siblings. Arthritis & Rheumatism 39:904–913.

Tong J, Allenspach EJ, Takahashi SM, Mody PD, Park C, Burkhardt JK, Sperling AI. 2004. CD43 regulation of T cell activation is not through steric inhibition of T cell-APC interactions but through an intracellular mechanism. The Journal of Experimental Medicine 199:1277–1283.

Wack A, Cossarizza A, Heltai S, Barbieri D, D'Addato S, Fransceschi C, Dellabona P, Casorati G. 1998. Age-related modifications of the human alphabeta T cell repertoire due to different clonal expansions in the $CD4^+$ and $CD8^+$ subsets. International Immunology 10:1281–1288.

Weng NP. 2006. Aging of the immune system: How much can the adaptive immune system adapt? Immunity 24:495–499.

Yamaoka M, Kusunoki Y, Kasagi F, Hayashi T, Nakachi K, Kyoizumi S. 2004. Decreases in percentages of naïve CD4 and CD8 T cells and increases in percentages of memory CD8 T cell subsets in the peripheral blood lymphocyte populations of A-bomb survivors. Radiation Research 161:290–298.

Radiation Research

Official Journal of the Radiation Research Society

Clonally Expanded T Lymphocytes from Atomic Bomb Survivors *In Vitro* Show No Evidence of Cytogenetic Instability

K. Hamasaki,[a,e] Y. Kusunoki,[a,e] E. Nakashima,[c] N. Takahashi,[b,e] K. Nakachi,[a] N. Nakamura[d] and Y. Kodama[b,e,1]

Departments of [a] Radiobiology and Molecular Epidemiology, [b] Genetics and [c] Statistics and [d] Chief Scientist, Radiation Effects Research Foundation, Minami-ku, Hiroshima, 732-0815, Japan; and [e] Hiroshima University Graduate School of Biomedical Sciences, Minami-ku, Hiroshima 734-8551, Japan

RADIATION RESEARCH 172, 234–243 (2009)
0033-7587/09 $15.00

DOI: 10.1667/RR1705.1

Clonally Expanded T Lymphocytes from Atomic Bomb Survivors *In Vitro* Show No Evidence of Cytogenetic Instability

K. Hamasaki,[a,e] Y. Kusunoki,[a,e] E. Nakashima,[c] N. Takahashi,[b,e] K. Nakachi,[a] N. Nakamura[d] and Y. Kodama[b,c,1]

Departments of [a] Radiobiology and Molecular Epidemiology, [b] Genetics and [c] Statistics and [d] Chief Scientist, Radiation Effects Research Foundation, Minami-ku, Hiroshima, 732-0815, Japan; and [e] Hiroshima University Graduate School of Biomedical Sciences, Minami-ku, Hiroshima 734-8551, Japan

Hamasaki, K., Kusunoki, Y., Nakashima, E., Takahashi, N., Nakachi, K., Nakamura, N. and Kodama, Y. Clonally Expanded T Lymphocytes from Atomic Bomb Survivors *In Vitro* Show No Evidence of Cytogenetic Instability. *Radiat. Res.* 172, 234–243 (2009).

Genomic instability has been suggested as a mechanism by which exposure to ionizing radiation can lead to cancer in exposed humans. However, the data from human cells needed to support or refute this idea are limited. In our previous study on clonal lymphocyte populations carrying stable-type aberrations derived from A-bomb survivors, we found no increase in the frequency of sporadic additional aberrations among the clonal cell populations compared with the spontaneous frequency *in vivo*. That work has been extended by using multicolor FISH (mFISH) to quantify the various kinds of chromosome aberrations known to be indicative of genomic instability in cloned T lymphocytes after they were expanded in culture for 25 population doublings. The blood T cells used were obtained from each of two high-dose-exposed survivors (>1 Gy) and two control subjects, and a total of 66 clonal populations (36 from exposed and 30 from control individuals) were established. For each clone, 100 metaphases were examined. In the case of exposed lymphocytes, a total of 39 additional *de novo* stable, exchange-type aberrations [translocation (t) + derivative chromosome (der)] were found among 3600 cells (1.1%); the corresponding value in the control group was 0.6% (17/3000). Although the ratio (39/3600) obtained from the exposed cases was greater than that of the controls (17/3000), the difference was not statistically significant ($P = 0.101$). A similar lack of statistical difference was found for the total of all structural chromosome alterations including t, der, dicentrics, duplications, deletions and fragments ($P = 0.142$). Thus there was no clear evidence suggesting the presence of chromosome instabilities among the clonally expanded lymphocytes *in vitro* from A-bomb survivors.

[1] Address for correspondence: Departments of Genetics, Radiation Effects Research Foundation, 5-2 Hijiyama Park, Minami-ku, Hiroshima 732-0815, Japan; e-mail: ykodama@rerf.or.jp.

INTRODUCTION

Radiation-induced genomic instability has been defined as events that occur in cells many generations after irradiation and that are distinguishable from the immediate effects of radiation. In 1992, Kadhim *et al.* (*1*) reported elevated frequencies of non-clonal *de novo* chromosome aberrations (mainly chromatid-type aberrations) in *in vitro* cultures of mouse hematopoietic stem cells irradiated *in vivo* with α particles. A number of delayed effects after exposure to both high- and low-LET radiation have since been described. It is now recognized that instability can be measured using not only chromosome alterations as a marker but also other end points such as gene mutations and cell death [see refs. (*2–5*) for reviews]. Genomic instability induced by radiation has been proposed to be an early event associated with the initiation of carcinogenesis (*6*). This model has therefore attracted many investigators interested in radiation-induced cancer.

While there are many reports describing radiation-induced genomic instability, only a few studies have been done with human cells, and the results are not concordant. Holmberg *et al.* (*7*) reported that the clonal descendants of X-irradiated human T lymphocytes acquired new stable-type aberrations 16–62 days after *in vitro* culture. In studies of people accidentally exposed to ^{137}Cs γ rays, Salomaa *et al.* (*8*) observed a significant increase in the frequency of exchange-type aberrations, including dicentrics (dic) in long-term lymphocyte cultures. Hofman-Huther *et al.* (*9*) observed an increased frequency of unstable-type aberrations (dic) at 8–41 days after the irradiation of human lymphocytes with X rays or 100 MeV/nucleon carbon ions. Similarly, delayed chromosome aberrations were reported in cultured human fibroblasts (*10–13*) and in human bone marrow cells (*14*). In contrast, Tawn *et al.* (*15*) examined lymphocytes from radiotherapy patients 6–60 months after their treatments and found no evidence for extended instabilities. Whitehouse and Tawn (*16*) did not detect any increase in the frequency of delayed chromosome alterations in the lymphocytes of radiation workers

exposed to plutonium. Furthermore, Dugan and Bedford (*17*) used low-passage normal primary diploid fibroblasts to measure induction of delayed chromosomal instability after irradiation and found no clear evidence for it. Observations of instabilities in normal human cells are therefore inconsistent; thus the question remains as to whether instability can occur in the cells of people exposed to radiation *in vivo*.

We previously examined the possibility of radiation-induced delayed chromosome aberrations in A-bomb survivors using the frequency of additional *de novo* translocations among clonally expanded T lymphocytes *in vivo* as an indicator (*18*). The results indicated that the frequency of new translocations among the clonal populations in A-bomb survivors was not higher than the frequency among non-clonal cells from controls, indicating a lack of instability *in vivo*. We concluded that radiation-induced chromosome instability is not as common as an increased frequency of translocations among clonally derived lymphocytes.

In the present work, the earlier study was extended by clonally expanding T cells from A-bomb survivors to determine whether chromosome instability can develop during long-term culture *in vitro*. Two proximally exposed A-bomb survivors were selected for the study because both were known to bear clonal chromosome aberrations with a high frequency (*18*). Since the frequencies of these clones were 10% and 50%, respectively, among the blood lymphocytes, the clonally derived cells must have proliferated extensively *in vivo*. Thus we anticipated that such clonal cells may exhibit significant induction of chromosome instability after long-term forcible cell proliferation *in vitro*. Multicolor FISH (mFISH) was used to detect newly arisen non-clonal chromosome aberrations that may occur in those clones. T-cell clonal populations from age- and sex-matched control individuals were also studied for comparison.

MATERIALS AND METHODS

Blood Donors

Peripheral blood lymphocytes were obtained from four female A-bomb survivors (cases 1–4). Table 1 gives information about the subjects. Briefly, cases 1 and 2 were survivors exposed to large doses of radiation (more than 1 Gy). Both were known to carry clonal chromosome aberrations with a high frequency (*18*). Cases 3 and 4 were survivors whose estimated doses were less than 5 mGy; they were selected as age- and sex-matched controls for cases 1 and 2, respectively. None of the donors had a medical history of cancer before blood was drawn.

These survivors belong to the Adult Health Study (AHS) cohort at the Radiation Effects Research Foundation (RERF) in Hiroshima (*19*). Their radiation doses were estimated using the Dosimetry System 2002 [DS02; ref. (*20*)]. A fixed weighting factor of 10 was used for neutrons to calculate the weighted total dose in Gy (*21*). This study is a part of our extensive research program for biological dose estimations for AHS individuals and was approved by the program review committee and the ethical review committee at RERF.

Lymphocyte Cloning and Culture

Peripheral blood mononuclear cells (PBMCs) were separated by Ficoll-Hypaque (LSM, Lymphocyte Separation Medium; MP Biomedicals, Aurora, OH) density gradient centrifugation. T lymphocytes were cloned and expanded *in vitro* by methods described elsewhere (*22*) with some modifications. PBMCs at a mean frequency of 0.5 cell/well were distributed into each well of a 96-well round-bottom plate (Corning, Corning, NY). GIT medium (Wako Pure Chemical Industry, Osaka, Japan) containing 9% fetal bovine serum (FBS; Intergen, New York, NY), 1% human AB-type serum, 2% L-glutamine (Invitrogen, Carlsbad, CA), 2% penicillin-streptomycin (Invitrogen), 1:6400 phytohemagglutinin (PHA; Difco Laboratories, Detroit, MI), and 10 ng/ml recombinant human interleukin 2 (rhIL-2; Pepro Tech, London, UK), was used. Feeder cells (5×10^4 allogeneic PBMCs and 10^4 lymphoblastoid cells, OKIB, irradiated with 50 and 100 Gy of X rays, respectively) were added. After about 2 weeks of incubation at 37°C in a humidified 5% CO_2/95% air incubator, each growing colony was transferred into one well of a 24-well plate (Corning) with the same culture medium containing 2.5×10^4 beads/ml of CD3/CD28 T-cell expander beads (Dynal Biotech ASA, Oslo, Norway) and cultured until several million cells were obtained. For cases 2, 3 and 4, the average culture time was approximately 4 weeks, and the number of population doublings was 23 to 25. In case 1, T-cell colonies that had been cloned previously (*22*) and cryopreserved were thawed and cultured in a 24-well plate under the same culture conditions.

mFISH Analysis

Chromosome slides were prepared by conventional air-drying methods 2 h after treatment of the cultured cells with colcemid (100 ng/ml) (*23*). mFISH was performed with SpectraVision DNA probes (Vysis, Downers Grove, IL) according to the manufacturer's protocol (*24*). The probes were denatured and hybridized to metaphase spreads at 37°C for two nights (~42 h). The slides were then washed in 0.4× SSC/0.3% NP-40 at 73°C for 2 min followed by a 2× SSC/0.1% NP-40 wash at room temperature for 1 min and finally a 2× SSC wash at room temperature for 2 min before subsequent application of a mounting medium (4′,6-diamidino-2-phenylindole, DAPI, 250 ng/ml) and a cover slip. Acquisition and analysis of mFISH images was performed using a CytoVision ChromoFluor System (Applied Imaging, Newcastle upon Tyne, UK). One hundred cells were scored for each clone.

Hematopoietic Colonies

As described elsewhere (*21*), approximately 500 CD34 (a hematopoietic stem cell surface marker) -positive cells were sorted from about 2 million PBMCs using a cell sorter (JSAN, Bay Bioscience, Kobe, Japan) and resuspended in 0.2 ml Iscove's MDM (Invitrogen) containing 2% FBS. The cell suspension was mixed with 2 ml methylcellulose medium (Methocult TM GF H4434V; Stemcell Technologies, Vancouver, Canada) containing recombinant human (rh) erythropoietin, rh stem cell factor, rhGM-CSF, rhG-CSF and rhIL-3 and then dispensed into two 35-mm petri dishes (about 1.1 ml each). After 10 days in culture at 37°C in 5% CO_2, the cells were treated with 100 ng/ml colcemid for 16 h and collected for chromosome analyses.

RESULTS

Characteristics of T-Cell Clones Obtained from the Peripheral Blood of A-Bomb Survivors

A total of 66 clones were established from two A-bomb survivors and two control individuals (see Table 1).

TABLE 1
Summary of the Study Subjects

Case no.	Sex	Age at the time of bombing (years)	Age when blood samples were collected (years)	DS02 bone marrow dose (mGy)	Blood sample used for the study	Information about *in vivo* clonal aberrations
1	F	20	65	1950	Frozen blood (16 years)[a]	Clone with t(4;6),t(5;13) in ~10% of the cells
2	F	13	72	1150	Freshly obtained blood	Clone with t(2;4) in ~50% of the cells
3	F	19	63	1.3	Frozen blood (17 years)[a]	No clone
4	F	13	70	1.7	Frozen blood (2 years)[a]	No clone

[a] Numbers in parentheses indicate the length of time the blood samples were kept in liquid nitrogen.

Case 1. This survivor had been exposed to a large dose of radiation (estimated dose is 1.95 Gy). Cells from this individual are known to bear an identical double translocation [t(4;6),t(5;13)] in about 10% of the lymphocytes (*18*). In the present experiments, 14 clones were studied that had been isolated and frozen 16 years ago (*22*). These consisted of four clones with a normal karyotype five with identical double translocations [t(4;6),t(5;13)] derived from the clonal cells *in vivo*, four with different structural aberrations, and one with mosaic X chromosome aneuploidy (45,X/46,XX) (Table 2).

Case 2. This person had been exposed to a large dose of radiation (estimated dose is 1.15 Gy). Cells from this person are also known to carry a clonal population of blood lymphocytes with high percentage of the clonal translocations, i.e., [t(2;4)] in about 50% of the cells (*18*). Twenty-two clones were obtained including eight clones with normal karyotypes, eight with the clonal translocations [t(2;4)], five with other structural aberrations, and one with a chromosome 2 trisomy (Table 3).

Case 3. This donor was selected as an age- and sex-matched control for Case 1. Of the 12 clonal cell populations obtained, 10 clones had a normal karyotype, one had a deletion of chromosome 5q, and one was mosaic for X chromosome aneuploidy (45,X/47,XXX) (Table 4).

Case 4. This donor was selected as an age- and sex-matched control for Case 2. Eighteen clones were obtained, of which 14 clones had a normal karyotype, two had a monosomy for the X chromosome, one had a chromosome 22 trisomy, and one had a mosaic X chromosome aneuploidy (45,X/46,XX/47,XXX) (Table 5).

Origin of Clonal Chromosome Aberrations In Vivo

The origin of the clonal chromosome aberration in case 1 [t(4;6),t(5;13)] was previously confirmed as deriving from a single bone marrow stem cell, because identical double translocations were observed not only in peripheral blood lymphocytes (both T and B) but also in stem cell-derived BFU-E colonies (*22*). In case 2, the identical translocations [t(2;4)] were detected in both CD4 and CD8 T-lymphocyte populations (*25*), but no further examination had been done. In the present study, CD34-positive cells were cultured from blood mononuclear cells, and a t(2;4) translocation was found in nearly 80% of the metaphases examined (156/200) with the FISH method

TABLE 2
Frequency of Additional Chromosome Aberrations among Clonally Expanded T Lymphocytes *In Vitro* in Case 1

			Additional chromosome aberrations[a]								
			Structural aberrations							Aneuploidy	
Clone no.	Karyotype	No. of cells examined	t	der	dic	dup	del	f	total	gain	loss
1-1	46,XX	100		1		1	3	1	6		8
1-2	46,XX	100	1				1	2	4	1	3
1-3	46,XX	100					1	6	7		2
1-4	46,XX	100						1	1		3
1-5	45,X/46,XX	86/14				1	3		4	1	5
1-6	t(4;6),t(5;13)	100	3	1		5 (4)	21 (9)	4	21	6 (4)[b]	10
1-7	t(4;6),t(5;13)	100		3				3	6		3
1-8	t(4;6),t(5;13)	100			1		2	2	5	3	3
1-9	t(4;6),t(5;13)	100				1	1		2	1	2
1-10	t(4;6),t(5;13)	100		3 (2)					2		3
1-11	t(X;2),t(5;12),t(6;11;10)	100	1			3 (2)	2		5	3	7
1-12	t(7;12)	100					2	1	3		5
1-13	t(3;21)	100			1			1	2	1	3
1-14	t(3;6;12)	100					1	2	3	3	5
	Total	1400	5	7	2	9	25	23	71	17	62

Note. t = translocation, der = derivative chromosome, dic = dicentric chromosome, dup = duplication, del = deletion, f = fragment, gain = gain of chromosome, loss = loss of chromosome.

[a] Number in parentheses indicates the number of events (see the Results for details).

[b] An extra identical aberration [+del(1)(p11)] was detected in three cells.

TABLE 3
Frequency of Additional Chromosome Aberrations among Clonally Expanded T Lymphocytes *In Vitro* in Case 2

Clone no.	Karyotype	No. of cells examined	Additional chromosome aberrations								
			Structural aberrations							Aneuploidy	
			t	der	dic	dup	del	f	total	gain	loss
2-1	46,XX	100		2			2	3	7	4	9
2-2	46,XX	100	1				1		2	1	7
2-3	46,XX	100		1					1	3	3
2-4	46,XX	100						2	2	2	8
2-5	46,XX	100	1				2	1	4	3	14
2-6	46,XX	100					3	4	7	1	9
2-7	46,XX	100	1				6	2	9	1	6
2-8	46,XX	100	3	1			3		7		3
2-9	47,XX,+2	100	1	1			4		6	1	10
2-10	46,XX,t(2;4)	100	1			7 (1)	1	2	5	4	8
2-11	46,XX,t(2;4)	100					2	1	3	2	1
2-12	46,XX,t(2;4)	100	1				5		6	2	10
2-13	46,XX,t(2;4)	100	1				2	7	10	4	4
2-14	46,XX,t(2;4)	100	1		1		2		4	1	3
2-15	46,XX,t(2;4)	100	1	1		1	4	1	8	2	10
2-16	46,XX,t(2;4)	100		9 (2)			1	1	4		3
2-17	46,XX,t(2;4)	84					1		1	4 (1)[a]	6
	46,XX,t(3;22), t(4;8)	16							0		
2-18	46,XX,t(1;10)	100	1	1			3	1	6	3	11
2-19	46,XX,t(1;12)	100	2		1		1	1	5	1	3
2-20	47,XXX,t(13;18;20)	100		3	18		2	1	24	6	2
2-21	45,X, t(2;8;17)	100					2		2	2	9
2-22	45,X,t(2;16)	100					1	1	2	1	3
	Total	2200	15	12	20	2	48	28	125	45	142

Note. Abbreviations are defined in Table 2.
[a] Extra derivative chromosome [+der(2)] that is the counterpart of an *in vivo* clonal translocation was detected in 4 cells.

using probes specific for chromosomes 2 (Green) and 4 (Red). We thus concluded that the t(2;4) clone in case 2 derived from a hematopoietic stem cell.

Additional Chromosome Aberrations Detected in Clonally Expanded T Lymphocytes

Data for individual clones from each blood donor are shown in Tables 2–5. Various types of new "additional" aberrations were detected among the 100 cells from the clones examined. Further, identical aberrations were frequently encountered in multiple cells in the population of clonal cells. Since these aberrations almost certainly arose only once during clonal culture *in vitro*, each identical aberration was counted as a single event. The numbers in parentheses in Tables 2–5 indicate the number of such events (intraclonal clones or subclonal clones).

TABLE 4
Frequency of Additional Chromosome Aberrations among Clonally Expanded T Lymphocytes *In Vitro* in Case 3

Clone no.	Karyotype	No. of cells examined	Additional chromosome aberrations								
			Structural aberrations							Aneuploidy	
			t	der	dic	dup	del	f	total	gain	loss
3-1	46,XX	100					2	2	4		4
3-2	46,XX	100					1	1	2	2	4
3-3	46,XX	100				1	2		3	2	4
3-4	46,XX	100	1	3			1		5	3	4
3-5	46,XX	100	1	1			2	4	8		8
3-6	46,XX	100							0		3
3-7	46,XX	100				1	3	4	8	1	4
3-8	46,XX	100				1	1	3	5		4
3-9	46,XX	100	1	7 (4)				1	6	2	1
3-10	46,XX	100							0	1	5
3-11	45,X/47,XXX	35/65							0		3
3-12	46,XX,del(5q)	100					2		2	5	4
	Total	1200	3	8	0	3	14	15	43	16	48

Note. Abbreviations are defined in Table 2.

TABLE 5
Frequency of Additional Chromosome Aberrations among Clonally Expanded T Lymphocytes *In Vitro* in Case 4

Clone no.	Karyotype	No. of cells examined	Additional chromosome aberrations								
			Structural aberrations							Aneuploidy	
			t	der	dic	dup	del	f	total	gain	loss
4-1	46,XX	100					5	6	11	3	3
4-2	46,XX	100		1		1	2	2	6	2	6
4-3	46,XX	100		1			1		2	1	5
4-4	46,XX	100					3		3	3	5
4-5	46,XX	100					2		2		10
4-6	46,XX	100					11 (6)	3	9	4	1
4-7	46,XX	100					1	1	2		5
4-8	46,XX	100						2	2		6
4-9	46,XX	100	1						1	3	2
4-10	46,XX	100					2	3	5	1	4
4-11	46,XX	100					1		1	1	4
4-12	46,XX	100					1	2	3	5	4
4-13	46,XX	100					3	1	4	1	4
4-14	46,XX	100	1		1		10 (5)	1	8	5	5
4-15	45,X	100					3	2	5	2	7
4-16	45,X	100	2		1	2	3 (2)	2	9	1	6
4-17	47,XX,+22	100					2		2	3	1
4-18	45,X/ 46,XX /47,XXX	80/3/17					1		1		8
	Total	1800	4	2	2	3	40	25	76	35	86

Note. Abbreviations are defined in Table 2.

Most of the clonal populations we observed appeared to be of single cell origin except for four clones; clone no. 2-17 appears to have started with two cells instead of one. The other three clones (nos. 1-5, 3-11, 4-18) consisted of cells with X-chromosome aneuploidy. Although it is not possible to determine whether they were derived from multiple cells or were the result of sex-chromosome loss or non-disjunction during clonal expansion, the latter possibility appears to be more likely since X-chromosome aneuploidy is known to take place commonly in cultured lymphocytes from elderly women (*26*). The above three X-chromosome aneuploid clones, together with two other clones, that showed autosomal trisomy (nos. 2-9, 4-17) were categorized as a "normal karyotype" in Table 6.

Statistical Analyses of the Additional Chromosome Aberration Frequencies in Exposed and Control Subjects

1. Reciprocal translocations (t)

It is generally thought that since reciprocal translocations do not gain or lose DNA, they are not subject to negative selection that would result in their reduced fraction during extensive cell divisions (*27*). Therefore, if reciprocal translocations had been induced by genomic instability they must have accumulated among descendant cells during *in vitro* culture of the clones. The frequency of newly induced additional reciprocal translocations (t) in the exposed subjects (cases 1 and 2) was 0.56% (20/3600), whereas it was 0.23% (7/3000) in the controls (cases 3 and 4) (Table 6). This difference is not statistically significant ($P = 0.070$) with the Wald test using the quasi-likelihood method. This same statistical evaluation was applied in the following section.

2. Derivative chromosome (der)

An example of derivative chromosomes is shown in Fig. 1b. These chromosomes are composed of non-reciprocal translocations and hence are accompanied by gains and losses of DNA segments that may confer a growth disadvantage to the cells. They seem to arise as a result of chromatid-type exchanges in S phase. The frequency of derivative chromosomes was 0.53% (19/3600) in the exposed cases, and 0.33% (10/3000) in the controls (Table 6). The difference was not statistically significant ($P = 0.371$).

mFISH is recognized as the best technique available for the detection of interchromosomal exchanges such as translocations and derivative chromosomes described here. Since both translocations and derivative chromosomes are stable-type aberrations and thus can be transferred to the next generation, the combined data for (t + der) were also analyzed. The results indicated no statistically significant difference between the two groups ($P = 0.11$).

3. Dicentric chromosomes (dic)

Dicentric chromosomes, or dicentrics, are representative of unstable-type chromosome aberrations that are easily detected but are lost over time during successive cell divisions due to problems associated with mitotic chromosome segregation. Consequently, it is generally thought that such aberrations do not accumulate in a cell population. As shown in Tables 2–5, the dicentric frequencies observed in the subjects were 0.1% (2/1400, case 1), 0.9% (20/2200, case 2), 0% (0/1200, case 3), and 0.1% (2/1800, case 4), respectively. Three cases (1, 3, 4) had

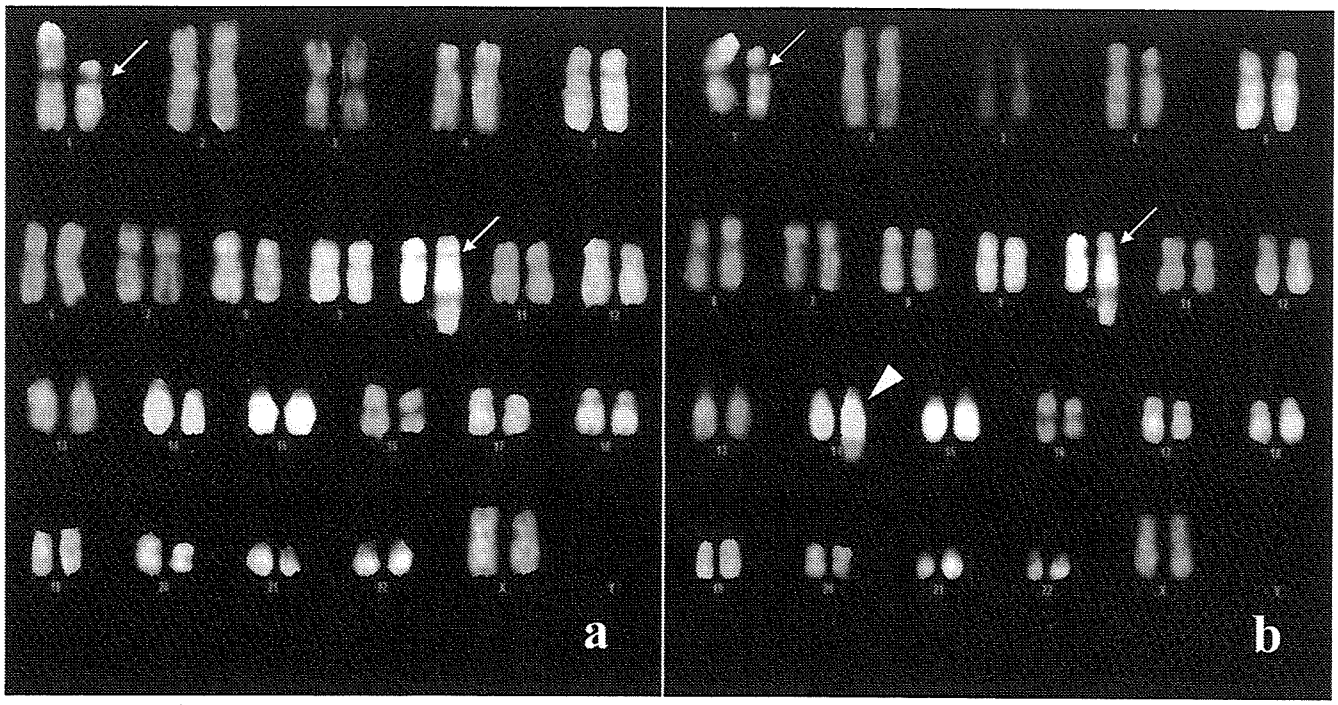

FIG. 1. Detection of additional chromosome aberrations with mFISH (Clone 2-18 in Table 3). Panel a: Translocation alone, 46,XX,t(1;10). Panel b: Translocation plus non-clonal aberration, 46,XX,t(1;10),der(14)t(2;14). Arrows indicate the translocation between chromosomes 1 and 10 and the arrowhead shows the additional aberration (derivative chromosome) involving chromosomes 2 and 14. Two normal intact number 2 chromosomes are evident.

relatively low levels of dicentric frequencies corresponding to control values when human blood lymphocytes were examined after short-term culture (0.1–0.2%) (*28*). However, clone 2-20 from case 2 developed a relatively high frequency of apparent dicentric chromosomes in the culture (18/100, Table 2). None, however, had accompanying fragments, which indicates that they resulted from the terminal fusion of two chromosomes (see Discussion). Six dicentrics were detected independently in other clones, some with fragments, and were considered to be true dicentrics since their breakpoints were distributed in non-terminal regions of the chromosomes. When clone 2-20 was excluded from the analysis, the dicentric frequency in case 2 was similar to those seen for samples from non-exposed controls (0.1%, 2/2100) (*28*).

4. Other aberrations (deletions, duplications, fragments and aneuploidy)

Although the mFISH technique is not highly sensitive for detecting structural chromosome aberrations such as duplications, deletions and fragments (i.e., without color change), some of those aberrations were clearly detectable with mFISH in combination with DAPI counterstaining. The numbers of such aberrations detected in this study are summarized in Table 6. The pooled frequencies of these three types of aberrations (dup + del + f) was 3.75% (135/3600) in the exposed cases and 3.33% (100/3000) in the controls. The difference between the two groups was not statistically significant ($P > 0.5$).

On the other hand, mFISH is the most reliable method for detecting aneuploidy, i.e. chromosome gains or losses in metaphase spreads. However, there was no statistically significant difference in the observed frequency of chromosome gain between the exposed (1.7%, 62/3600) and the control groups (1.7%, 51/3000) ($P > 0.5$). The observed frequency of chromosome loss was slightly higher in the exposed group (5.67%, 204/3600) than in the control group (4.47%, 134/3000), but again the difference was not statistically significant ($P = 0.069$). As shown in Table 6, the occurrence of chromosome loss was three times higher ($n = 338$) than that of chromosome gain ($n = 113$), which could indicate that some of the losses were due to artifacts that can occur during preparation of metaphase spreads (*29*).

5. All structural chromosome aberrations

The combined data for all structural chromosome aberrations of the exposed and the control groups were compared, and no statistically significant difference was observed ($P = 0.142$).

DISCUSSION

To investigate radiation-induced genomic instability in human peripheral blood lymphocytes, T lymphocytes from A-bomb survivors were clonally expanded *in vitro*, and the frequencies of additional *de novo* chromosome aberrations arising in individual clones during the

TABLE 6
Frequency of Karyotypes and Additional Chromosome Aberrations in T Cell *In Vitro* Clones from Exposed and Control Subjects as well as among Different Karyotypes

Karyotype of the clone[a]	No. of clones	Total cells	Additional chromosome aberrations		
			Structural aberrations		
			t	der	dic
Exposed (cases 1 + 2)					
Normal	14	1400	8 (0.57%)	6 (0.43%)	0 (0.00%)
In vivo-derived clonal aberration	13	1300	8 (0.62%)	9 (0.69%)	2 (0.15%)
Other structural aberrations	9	900	4 (0.44%)	4 (0.44%)	20 (2.22%)
Total[b]	36	3600	20 (0.56%)	19 (0.53%)	22 (0.61%)
Control (case 3 + 4)					
Normal	29	2900	7 (0.24%)	10 (0.34%)	2 (0.07%)
Other structural aberrations	1	100	0 (0.00%)	0 (0.00%)	0 (0.00%)
Total[b]	30	3000	7 (0.23%)	10 (0.33%)	2 (0.07%)

[a] Clones with aneuploid karyotypes were classified as "Normal". t = translocation, der = derivative chromosome, dic = dicentric chromosome, dup = duplication, del = deletion, f = fragment, gain = gain of chromosome, loss = loss of chromosome.
[b] Numbers in total indicate the number of events.

cultivation period were determined with mFISH. The results did not provide any conclusive evidence for the presence of chromosome instability, although the observed frequency estimate was slightly higher in the exposed cases. The results are therefore in accord with our previous study in which no increased levels of chromosome instability were found in clonally expanded lymphocyte populations *in vivo* in A-bomb survivors (*18*). Our previous *in vivo* and present *in vitro* observations will raise a question about the general involvement of chromosome instability as an initiating step in radiation-induced carcinogenesis.

In Vivo Clonal Chromosome Aberrations

As described in the Results section, the clonal chromosome aberrations observed in a large number of cells from case 1 and case 2 were both confirmed as being derived from aberrant bone marrow stem cells. It was previously found that these clones were induced after exposure to A-bomb radiation (*18*); thus the stem cells and their progenitors must have divided extensively. Nonetheless, the spontaneous frequency of new aberrations among the clonal cell populations was not much different from that in the control individuals (P = 0.114 for t + der and P = 0.13 for total structural aberrations). This may indicate that age-related increases in the frequency of chromosome aberrations in blood lymphocytes may not be due to an increased number of cell divisions of the stem/progenitor cells but rather to the systemic physiological conditions in the host (*18*).

Derivative Chromosomes

With the mFISH technique, it was possible to accurately identify chromosome aberrations such as derivative chromosomes (der) and duplications (dup) as additional aberrations in metaphase. Such aberrations are unusual in short-term cultures of lymphocytes (i.e., 2–3 days), which are used for standard human chromosome tests. In particular, derivative chromosomes are observed only rarely in normal cells, partly because their correct identification is very difficult with conventional cytogenetic techniques other than mFISH. In the present study, derivative chromosomes could be observed clearly in both exposed and control subjects, and there was no statistically significant difference in frequency between the two groups (P = 0.371). Therefore, it appears likely that most of these rare aberrations occurred during the long-term culture of the lymphocytes regardless of previous radiation exposure. In contrast to our results, Holmberg *et al.* described the appearance of derivative (or marker) chromosomes in human lymphocytes that were irradiated with X rays and subjected to long-term culture *in vitro* (*7*). This discrepancy might be attributed to either the single blood donor used for the Holmberg study and/or possibly suboptimal culture conditions for T lymphocytes because the rhIL2 used in the present study was not available in the 1980s when the Holmberg study was conducted.

One Apparently Unstable Clone with Possible Telomere Shortening

In clone no. 2-20 (case 2), 18 dicentric chromosomes were observed, and none of them contained acentric fragments. DAPI banding (counterstaining for mFISH) indicated that most of these dicentrics appeared to be end-to-end fusions of whole chromosomes. Further FISH analysis with pantelomere probes showed one telomere signal at each point of chromatid fusion (data not shown), suggesting a telomere-telomere fusion as a result of telomere shortening in at least some of the